ELSEVIER

Journal of Magnetism and Magnetic Materials 212 (2000) 307–322

Journal of magnetism and magnetic materials

www.elsevier.com/locate/jmmm

Interrelation of morphology, structure, and magnetism in Fe_xCo_{1-x}/Cu(1 0 0) epitaxial alloy films

A. Dittschar[a], W. Kuch[a,*], M. Zharnikov[b], C.M. Schneider[c]

[a]*Max-Planck-Institut für Mikrostrukturphysik, Weinberg 2, D-06120 Halle, Germany*
[b]*Universität Heidelberg, Angewandte Physikalische Chemie, D-69120 Heidelberg, Germany*
[c]*Institut für Festkörper- und Werkstofforschung Dresden, Helmholtzstr. 20, D-01069 Dresden, Germany*

Received 6 August 1999; received in revised form 30 November 1999

Abstract

Structure, morphology, and magnetism of epitaxial Fe_xCo_{1-x} alloy ultrathin films grown on Cu(1 0 0) in ultrahigh vacuum were investigated by a multi-technique approach over the whole composition range up to thicknesses of nine atomic monolayers (ML). Combining the results of the different techniques it is found that the films grow at room temperature in a distorted FCC structure with random chemical order. The amount and sign of the distortion depend on thickness and composition. Below $\approx$ 60 to 70% Fe content the alloy films are smooth, and exhibit two different vertical interlayer distances. At higher Fe concentrations several superstructures are observed, which are attributed to regular structural rearrangements. The structural relaxation above 4 ML thickness known from pure Fe films is not observed in the FeCo alloy films. Instead a gradual structural change towards a BCC(1 1 0) structure with increasing thickness occurs at higher Fe concentrations, and is still not complete in films as thick as 9 ML. The interrelation between morphology and structure in Fe_xCo_{1-x}/Cu(1 0 0) is discussed in terms of composition-dependent lattice parameters and strain. An expansion of the films in the plane leads to a stabilization of the FCC structure, whereas a compression leads to corrugated films with a tendency towards structural transformations. The absence of the relaxed FCC structure found in pure Fe films is explained by Co atoms acting as defects in the FCC structure of the alloy films either in a geometrical sense and/or because of their different magnetic moment with respect to the Fe atoms in both ferromagnetic and antiferromagnetic configurations of FCC Fe.

PACS: 68.55. − a; 75.50.Bb; 75.70.Ak

Keywords: Structure; Thin films; Alloys

1. Introduction

One of the most interesting issues in ultrathin film magnetism is the interrelation between morphology, structure, and magnetism. Although a considerable amount of work on ultrathin films has gone into investigating each of these points individually [1,2], the interrelation between these parameters, in particular between magnetism and crystalline structure, is still under discussion. A recent example for the influence of structure on magnetism was given by Zharnikov et al. [3,4]. In Fe/Cu(1 0 0) films of four monolayers (ML)

* Corresponding author. Tel.: + 49-30-6392-4927; fax: + 49-30-6392-4984.
E-mail address: kuch@port.exp.bessy.de (W. Kuch)

0304-8853/00/$ - see front matter
PII: S0304-8853(99)00840-9

a structural transformation at a critical temperature of 320 K is tied to a change of the magnetic properties of the film, namely to a transition from a ferromagnetic to a non-ferromagnetic state. A less investigated subject is the influence of morphology on crystalline structure or vice versa. Different film morphologies as a consequence of different growth conditions such as temperature and deposition rate may be the main reason for the observed shifts of the onset thickness of the FCC to BCC structural transition in ultrathin Fe films [5–8]. The influence of enhanced surface roughness on the magnetic anisotropy of the films was amongst others investigated by Chappert et al. [9]. It was found that an enhanced roughness generally decreases the uniaxial anisotropy contributions. It is important to know the relevant parameters for the determination of the roughness itself. Several investigations, e.g., for Fe/Cu(1 0 0) [5,10–12], Fe/Cu_3Au(1 0 0) [6,7], or Co/Cu(1 0 0) [13,14] have shown that the growth temperature can play a major role, as does the deposition rate [15,16].

The effect of principal structural parameters, like the lattice constant of the film in relation to the substrate lattice (lattice mismatch), on the roughness developing in the growth process is more difficult to investigate. Up to now, mostly single element films have been investigated. In this situation the lattice parameter in the film can only be modified by growing onto a different substrate. The physical properties of the film will therefore change discontinuously with the lattice parameter. This makes it difficult, if not impossible, to recognize a general trend for the influence of the lattice parameter on the morphology or on the magnetization. For this kind of investigations one would like to continuously vary the lattice parameter of the films. We will show in this article that a convenient way to do so is to use a binary alloy thin film system. In this case a continuous variation of the film composition can lead to a continuous alteration of film properties such as the lattice parameter and the average magnetic moment, and thus facilitate the study of interrelations in the structural, morphological, and magnetic behavior.

We present a multi-method investigation to disentangle the possible relationships between structure, morphology, and magnetism in a heteroepitaxial thin film system. As a model system Fe_xCo_{1-x}/Cu(1 0 0) was chosen. There are two major reasons for this choice: On the one hand each of the single component films Fe/Cu(1 0 0) and Co/Cu(1 0 0) were investigated very thoroughly [3–5,10–15,17–43], so that they can serve as a reference. On the other hand, these systems show quite opposite behavior with respect to magnetism and structure, which can result in interesting properties in the related alloy films. In particular, the Fe films assume a magnetization perpendicular to the surface below a certain critical thickness of about 10 ML [11,12,17–22], whereas the easy axis of magnetization in Co/Cu(1 0 0) always lies in the plane of the film [23–26]. The structural properties of Fe and Co films are also different. Whereas both films initially grow in an FCC-like structure matching the lateral lattice constant of the substrate, the dependence of the film structure on thickness is quite different. Co films keep the FCC structure up to a large thickness [13,14,25–29]. This structure is compressed vertically with respect to pure Cu [27]. The strain in the films is nearly constant up to about 16 ML, and is then released via formation of dislocations, the films still keeps the FCC structure [30]. In contrast to this, Fe films on Cu(1 0 0) grown at RT undergo rather complex changes in their structure during growth. Up to ≈ 4 ML the entire film is vertically expanded with respect to Cu, having a complex FCC-like structure with sinusoidal reconstruction both in the plane of the film, and perpendicular to this plane [31,32]. Above 4 ML thickness the 'bulk' of the film relaxes to a nearly unstrained FCC structure, whereas the topmost layer still shows an expanded interlayer distance [33,34]. In these films no reconstruction perpendicular to the film plane is observed [33,34]. In even thicker films a structural transformation from FCC to BCC occurs around 10 ML thickness [10,35–37]. This structural transformation is commonly held responsible for the switching of the magnetization into the film plane. Scanning tunneling microscopy (STM) investigations have revealed that already for thinner Fe films below 5 ML BCC precipitates can be found [10,36], which then develop into BCC grains with increasing thickness. The occurrence of these precipitates may be considered as an important factor facilitating the transition

from the fully expanded film to the relaxed structure at 4 ML thickness. Although this transition is essentially driven by a film energy reduction through relieving the strain in the films, the BCC-precipitates can provide a practical mechanism to overcome the respective energy barrier acting as dislocations which are necessary to realize the mismatch between the relaxed film and the substrate. This transition is also affected by the morphology. Fe films grown at low temperature ($\approx$120 K, LT) on Cu(1 0 0) show a different behavior compared to that of room temperature grown (RT) films. Whereas the structure of the LT films is quite similar to that of the RT films up to $\approx$4 ML, the LT films do not show the transition to the relaxed FCC Fe structure above that thickness. Instead a direct transition to a (1 1 0) oriented BCC structure is observed between 3.2 and 5.8 ML thickness [5]. A possible reason for these structural peculiarities may be found in the different morphology of RT and LT Fe films. STM investigations have shown that LT films grow in small islands in contrast to a formation of large islands found for RT films [10,36].

Bulk FeCo alloys crystallize in various structural phases depending on the composition: at room temperature they assume the BCC structure over an extended composition range (25–100% Fe), but also FCC (5–10% Fe), HCP (0–5% Fe), and an BCC/FCC mixed phase are encountered (10–25% Fe) [44]. The magnetic moment of bulk BCC FeCo shows a maximum at about 70% Fe content [45,46].

In a previous short publication we have shown that Fe_xCo_{1-x} films grow on Cu(1 0 0) as chemically randomly ordered alloys in an FCC-like structure [47]. This was later confirmed by Tobin et al. [48,49]. In contrast to bulk BCC FeCo alloys no maximum of the magnetic moment as a function of composition was observed; instead, a nearly linear increase with increasing Fe content was found [47]. Preliminary measurements of the vertical interlayer distance of 5 ML thick Fe_xCo_{1-x} films have revealed that they depend on the composition of the films [47]. In a certain thickness range of FeCo/Cu(1 0 0) a composition-driven spin-reorientation transition from in-plane at lower Fe concentrations to perpendicular at higher Fe concentrations can be observed [50]. Here we extend these investigations by detailed low-energy electron diffraction (LEED), medium-energy electron diffraction during film growth (MEED), and magneto-optical Kerr-effect (MOKE) experiments, and combine the results obtained from the different methods to obtain a coherent picture of the structural, morphological, and magnetic properties of ultrathin Fe_xCo_{1-x}/Cu(1 0 0) films.

The organization of this paper is as follows: In Section 2 we will shortly describe the experimental setup. Detailed experimental results of LEED, MEED, and MOKE studies on Fe_xCo_{1-x} films are provided in Section 3. In the discussion (Section 4) we compare the experimental findings of the different techniques, and discuss how morphology, structure, and magnetism are related to each other in the Fe_xCo_{1-x} alloy system. At the end, the results are summarized in Section 5.

2. Experiment

Fe_xCo_{1-x} films were deposited onto a Cu(1 0 0) single-crystal substrate kept at room temperature (300 ± 5 K) in an ultrahigh vacuum chamber by Fe and Co co-evaporation from two separate sources. The growth process was monitored in situ by MEED, which allowed to control the film thickness with an accuracy of about 2–5%, and at the same time provided a means to judge the morphology of the films already during evaporation. In these MEED experiments, the specularly reflected intensity of a 2 keV primary electron beam at 3° grazing incidence in the [0 0 1] azimuth of the substrate was recorded as a function of evaporation time. The film composition was determined by Auger electron spectroscopy with an accuracy of 5% using calibration curves derived from pure Fe and Co films on Cu(1 0 0) [47]. The structural properties and the morphology of the films were investigated by LEED. The in-plane geometrical structure was extracted from LEED patterns, whereas the roughness of the films was judged from the intensity of the diffuse background. A fast kinematic analysis of LEED–$I(E)$ curves for the specularly reflected electron beam, incident at an angle of 7° to the surface normal in the (0 0 1) azimuth, allows one to

determine the average vertical lattice spacing for most of the films. Vertical lattice parameters of Fe/Cu(1 0 0) films measured this way [3,4], show a very good agreement when compared to more sophisticated, but also more time consuming fully dynamical LEED-analyses of several different LEED beams: In particular, in Fe films containing the relaxed FCC phase two coexistent vertical distances of 1.85 and 1.8 Å are found by the kinematic analysis [3,4], compared to 1.85 Å for the top layer distance, and varying layer distances from 1.81 to 1.77 Å in lower layers extracted from a full-dynamical LEED-analysis [38]. In 15 ML Ni films on Cu(1 0 0) the kinematic analysis yields 1.69 Å [51], which agrees exceptionally well with a fully dynamical analysis of 11 ML Ni/Cu(1 0 0) of Platow et al., where values between 1.690 and 1.700 Å have been found for the five topmost vertical layer distances [52]. As long as just the mean *vertical* atomic interlayer distance is concerned, we thus believe that the kinematic analysis of one LEED beam can in most cases provide values with a comparable accuracy as dynamic analyses.

Magnetic properties of the alloy films were probed by MOKE. MOKE measurements were performed in polar and longitudinal geometry [6,7] in a temperature range between 120 and 300 K. A more detailed description of the whole apparatus can be found elsewhere [4,53].

3. Results

Fig. 1 displays the variation of the intensity of the specularly diffracted (0 0) electron beam in the MEED experiments during evaporation of Fe_xCo_{1-x} films with different compositions. Up to an iron content of 60% the data shows pronounced oscillations starting at the second monolayer. This points towards good layer-by-layer growth and a smooth film surface after completion of each atomic layer. Further increasing the Fe content leads to a gradual damping of the intensity oscillations with increasing film thickness. The film thickness at which this damping starts decreases with increasing Fe content. It has to be emphasized that for $Fe_{92}Co_8$ and pure Fe films an astonishing difference between the intensity curves is found above

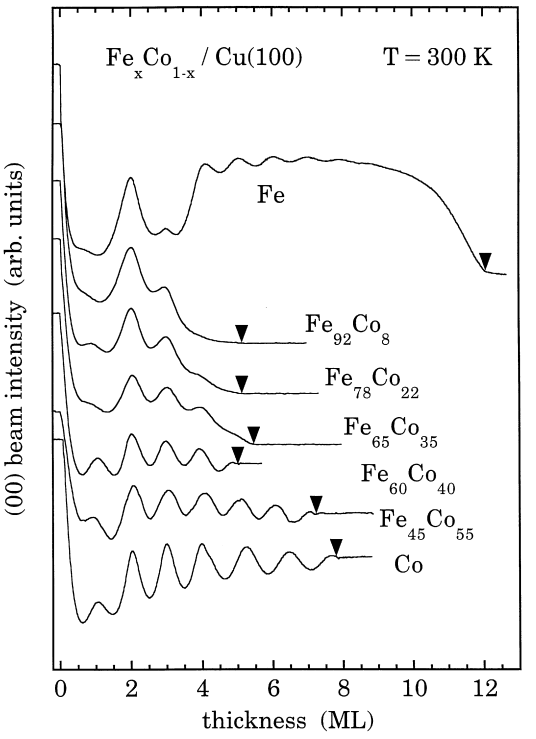

Fig. 1. Intensity of the specularly reflected MEED beam during evaporation. For a better display the curves are vertically offset. The triangles denote the end of evaporation.

3 ML film thickness, whereas both curves are virtually identical below this thickness. Associating a high MEED (0 0) beam intensity with a smooth surface, the films can be believed to be smooth over most of the concentration and thickness range investigated, except at Fe concentrations of $60\% \leqslant x < 100\%$ with thicknesses $d > 3.5$ ML.

This smoothness is confirmed by the low intensity of the LEED diffuse background. Fig. 2 shows LEED images of films with the thicknesses and compositions indicated at the respective panels. The diffuse background of the raw images is higher for films with high Fe content and large thicknesses, especially for films (d) (5 ML $Fe_{93}Co_7$) and (e) (9 ML $Fe_{90}Co_{10}$) (due to image processing the background of all images reproduced in Fig. 2 looks similar). For 4 ML $Fe_{86}Co_{14}$ (c) the background is already slightly higher than for the relatively thick 9 ML $Fe_{40}Co_{60}$ film (a). This is compatible to the MEED results, further

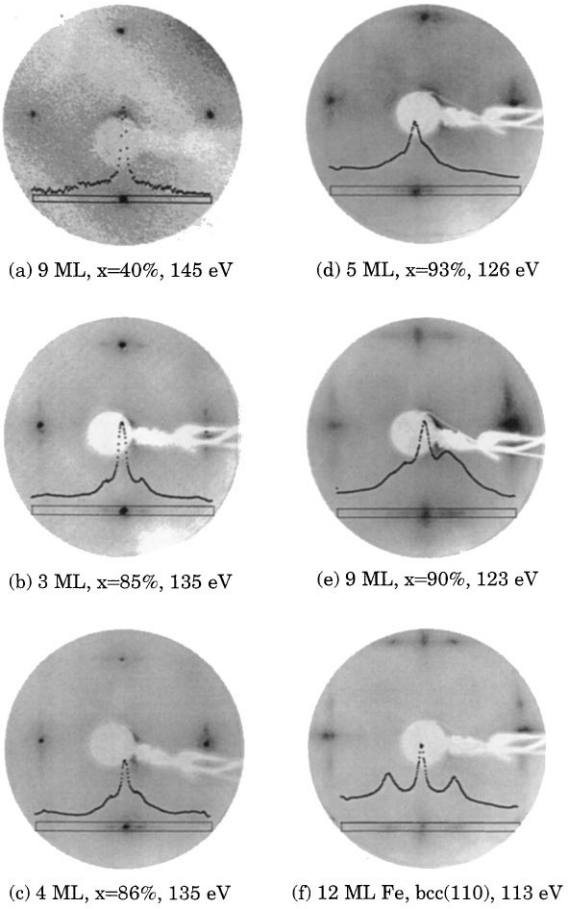

Fig. 2. LEED diffraction patterns for films of different thicknesses and compositions as indicated. The curves show the integrated intensity profile along the rectangular areas.

corroborating the interpretation in terms of smooth and rough film surfaces.

Line scans of the LEED intensity across the (0 $\bar{1}$) diffraction spot are plotted into the images to point out the superstructure spots. These linescans were obtained by summing the intensity over the width of the indicated rectangles. No superstructures are observed for the Fe_xCo_{1-x} films with Fe concentrations below $\approx$ 60–70%. As an example the 9 ML $Fe_{40}Co_{60}$ film can be taken. Like pure Co films [13,14,25,26,28], it shows a (1×1) structure. Very sharp spots are observed indicating a smooth film with good long-range crystalline order. For films with higher Fe content, for which the intensity in the MEED experiments starts to decrease at thicknesses $t > 3$ ML (cf. Fig. 1), several superstructures are observed. For 3 ML $Fe_{85}Co_{15}$, similar to pure Fe films of this thickness [31,32], (4×1) superstructure shows up (Fig. 2b). Not only this superstructure, but also the diffuse background of the $Fe_{85}Co_{15}$ film is very similar to that of pure Fe films of the same thickness. Going to 4 ML $Fe_{86}Co_{14}$, the superstructure changes to a (6×1) pattern, marked by a decreasing distance between the (0 $\bar{1}$) spot and the superstructure spots (Fig. 2c). This pattern is different to that of the corresponding thickness of pure Fe films, where a (5×1) superstructure is observed [32]. The background intensity, too, is higher for FeCo compared to pure Fe. Increasing further the thickness to 5 and 9 ML (Figs. 2d and e, respectively), the Fe_xCo_{1-x} films with $x = 93\%$ and 90% show a (7×1) and a (4×1) superstructure, respectively. At first sight the superstructure found for the 9 ML $Fe_{90}Co_{10}$ film looks very similar to the pattern of pure Fe films after the transition from FCC to BCC(1 1 0). The LEED pattern of such a film (12 ML Fe/Cu(1 0 0)) is presented in Fig. 2f. However, in addition to the fact that the background intensity of the 9 ML $Fe_{90}Co_{10}$ film is much higher than that of the 12 ML Fe film, one clearly observes distinct differences between the two intensity profiles. Whereas the profile of the 12 ML Fe film shows two clearly separated peaks, the intensity profile of the 9 ML $Fe_{90}Co_{10}$ film consists of two overlapping peaks on either side of the (1 0) diffraction spot with equal spacing between the additional peaks and the central (1 0) spot, corresponding to a (4×1) superstructure.

Summarizing the findings of the LEED experiments for different compositions, one can distinguish four regimes:

(i) $x \leqslant \approx 60\%$ with (1×1) structure,
(ii) $60\% \leqslant x \leqslant 100\%$ and $t < \approx$ 3–4 ML with (2×1) and (4×1) superstructures and relatively low background intensity,
(iii) $60\% \leqslant x < 100\%$ and $t > \approx$ 3–4 ML with increasing background intensity and (6×1), (7×1), and (4×1) superstructures, and
(iv) $x = 100\%$ and $t > \approx$ 3–4 ML with still low background intensity and (5×1) and (2×1) superstructures.

Let us next consider the vertical interlayer distances extracted from the $I(E)$ curves of the specular beam. We first keep the thickness of the films constant at 5 ML, and vary the composition. At this thickness we come across the area of low MEED beam intensity at high Fe concentrations, of high surface roughness, and pass several superstructures. After this we will focus on the development of the interlayer distances in films with a constant composition, namely $Fe_{85}Co_{15}$, upon changing the film thickness, and compare this with the results for pure Fe films.

For films with a fixed thickness of 5 ML some of the $I(E)$-curves used in the evaluation of the interlayer distances are shown in Fig. 3. A sequence of intensity maxima in the spectra can be associated with a certain interlayer distance. The energy positions of the maxima in such a sequence, shifted by the inner potential, are proportional to n^2/d^2, where d is the interlayer distance, and n an integer number [4]. Looking at Fig. 3 one can clearly identify these sequences of maxima. Compared to the clean Cu(1 0 0) surfaces the maxima related to the 5 ML Co film are shifted to higher energies corresponding to a smaller interlayer distance d. One can also see that, although the Co film is only 5 ML thick, the contribution of the Cu(1 0 0) substrate itself to the $I(E)$-spectrum is negligible. Adding Fe to the films, a shoulder on the lower energy side of the maxima found for pure Co emerges. The intensity of this shoulder increases with the Fe content, and develops into a new sequence of maxima. Above 70% Fe the sequence on the higher energy side, shaded dark, vanishes completely. Not only do the relative intensities of the two sequences of maxima change with the Fe content, but also shift both sequences to lower energies corresponding to larger average interlayer distances.

A possible explanation for two co-existing sequences of maxima/vertical interlayer distances would be a contribution from the substrate. However, the mean free path of the scattered electrons in the present energy range is quite small, and a substrate contribution in the 5 ML film can be excluded on the basis of the above argument, as is seen from Fig. 3. Consequently, a substrate contribution could show up only for a film with a very

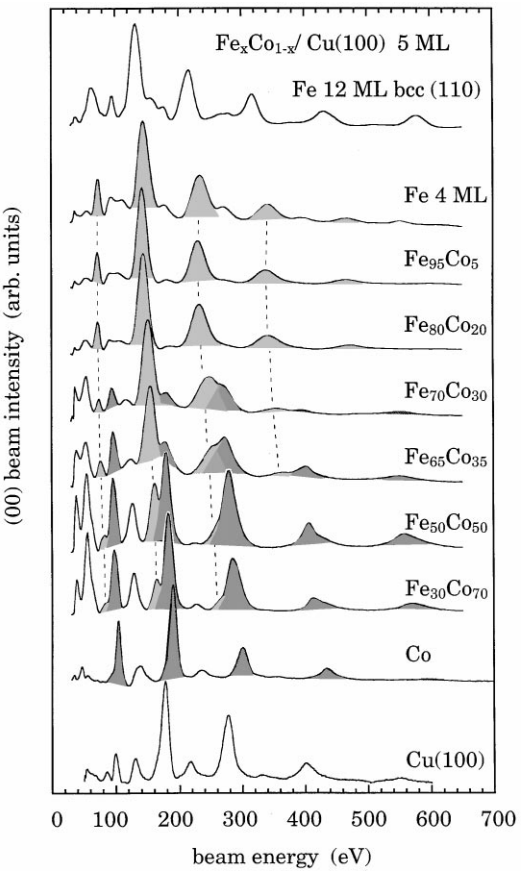

Fig. 3. $I(E)$ spectra for Fe_xCo_{1-x} films of different compositions but constant thickness of 5 ML, except for pure Fe where a 4 ML thick film was investigated. As a comparison the figure includes $I(E)$ spectra for the Cu substrate and a BCC(1 1 0) Fe film. The sequences of maxima belonging to a certain vertical interlayer distance are shaded light and dark.

inhomogeneous coverage, comprising regions of very thin film thickness. Such an inhomogeneous film thickness implies a high surface roughness, thereby resulting in low MEED intensities and a high intensity of diffuse background in the LEED image. None of this is observed for the films under discussion. The two sequences of maxima must therefore be related to the intrinsic structure of the FeCo film. Two possible geometrical arrangements may lead to the observed co-existence of different interlayer distances: (i) laterally confined regions with varying interlayer distances, or (ii) a vertical stacking of layers with the two distances. The first

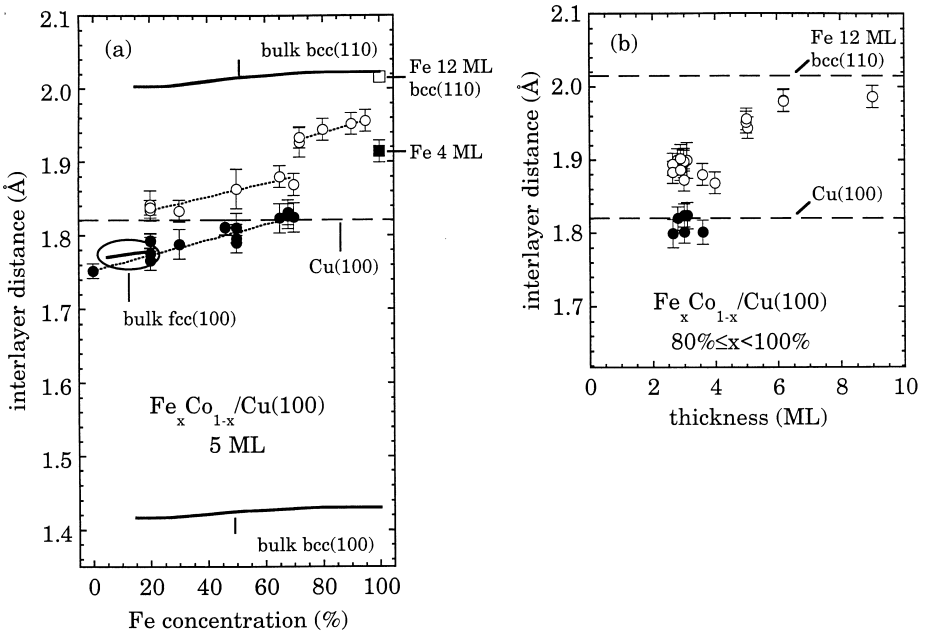

Fig. 4. Vertical interlayer distances calculated from LEED–$I(E)$ spectra of the specular beam. (a) Results for Fe_xCo_{1-x} films of 5 ML thickness (except pure Fe: 4 ML), and different compositions, (b) results for Fe_xCo_{1-x} films with $80\% \leqslant x < 100\%$ and different thicknesses. Additionally, the values of the Cu substrate and BCC(1 1 0) Fe films are indicated. The literature values for bulk FCC(1 0 0), BCC(1 0 0), and BCC(1 1 0) FeCo from Ref. [60] are reproduced as solid lines.

case implies a disalloying of Fe and Co resulting in areas with predominant Fe or Co content. In this case the increase of the intensity of the maxima of one component and the respective decrease of the intensity of the other component with film composition would suggest that the composition in both of these areas stays nearly constant, independent of the overall composition of the films. This should consequently result in two interlayer distances/sequences of maxima, the energetic position of which would be independent of the overall composition of the films. As can be seen in Figs. 3 and 4a, this is not the case. In fact, both sequences of maxima and hence both resulting interlayer distances show a smooth variation in energy and value, respectively. Therefore, arrangement (ii), namely a vertical stacking of different interlayer distances, is much more likely. A slight phase separation (segregation) of the Fe and Co atoms could still be present in that case. However, measurements of the angular distribution of the magnetic dichroism did not show any effects indicative of segregation of one of the components [54]. Also forward scattering of the Fe and Co LVV/Auger electrons from FeCo/Cu(1 0 0) films indicate a vertically regular distribution of both species, Fe and Co [55]. We thus conclude that a homogeneously mixed film of Fe and Co atoms is formed. This is plausible considering the similarity of the chemical bonds of metallic Fe and Co, and also the surface tensions of bulk Fe and Co, which are equal within 0.5% for both Fe and Co [56]. The observed two different vertical atomic interlayer distances are thus an intrinsic property of a chemically uniform film. Looking at the $I(E)$ spectra for $Fe_{50}Co_{50}$ and $Fe_{65}Co_{35}$ in Fig. 3, it is possible to decide which of the two vertical atomic distances $a_\perp$ is located at the substrate and which on the vacuum side. One clearly sees that the maxima of the lighter shaded sequence, corresponding to the larger $a_\perp$, dominate the maxima of the darker shaded sequence in the low-energy range; in the high-energy range, the

opposite behavior is observed. Because the mean free path of the higher energy electrons is larger than that of the low-energy electrons (about 4.7 ML at 500 eV compared to 1.7 ML at 50 eV [57]), the larger $a_\perp$ has to be located at the vacuum side of the film, whereas the smaller $a_\perp$ is located at the substrate interface of the film.

Such a vertical stacking of two different interlayer distances, or in other words, a vertical expansion of the topmost layers, is rather reasonable. For example, in Fe films on Cu(1 0 0) in the thickness range between 5 and 10 ML, the topmost layer shows a larger interlayer distance than the lower lying layers. The expansion or contraction of the topmost layers is in fact a well-known phenomenon. Especially in magnetic materials, where an additional magnetic energy contribution related to surface magnetic properties can come into play [58,59], this may be expected to manifest itself also in a structural differentiation between surface and bulk of a magnetic film.

Let us now consider the values of the vertical interlayer distances of the Fe_xCo_{1-x} films in more detail. The corresponding results are presented in Fig. 4. In Fig. 4a, the interlayer distances derived from the $I(E)$-curves for films of a constant thickness of 5 ML (except for pure Fe, where 4 ML are used) are presented together with literature values for Fe_xCo_{1-x} bulk materials [60]. It should be noted that for the clean Cu substrate the kinematic analysis of the $I(E)$ maxima yields a value of 1.82 Å, which is in good agreement with the results of dynamical LEED calculations [61], considering that the value from the kinematic analysis is only an average over the first few interlayer distances. Three different literature values for bulk FeCo are included in Fig. 4a in the respective relevant composition ranges. Above $\approx 15\%$ Fe, where a BCC structure is found for bulk Fe_xCo_{1-x}, we indicated the interlayer distances of BCC(1 0 0) and BCC(1 1 0) oriented planes of the crystal. Below $\approx 15\%$ Fe, where in the bulk an FCC structure is found, we only included the interlayer distances of the FCC(1 0 0) orientation. The experimental value for pure Co/Cu(1 0 0), and also the smaller $a_\perp$ value of the Fe_xCo_{1-x} films agrees very well with these numbers. Both interlayer distances found in the Fe_xCo_{1-x} films increase continuously with increasing Fe content. When extrapolating to $x = 1$ the larger one comes close to the respective value of the 4 ML Fe film. However, when the lower of the two interlayer distances of the Fe_xCo_{1-x} films approaches the value of the Cu substrate at $\approx 70\%$ Fe, a sudden increase in the value of $a_\perp$ occurs, and the two interlayer distances collapse to only one. We attribute this structural rearrangement to a different response of films under compressive and tensile strain, as will be discussed in the following section.

In Fig. 4b, the evolution of the interlayer distance of $Fe_{85}Co_{15}$ films as a function of film thickness is shown. Also here we observe two different values of $a_\perp$, although for this thickness (around only 3 ML) the smaller one may be feigned by the Cu substrate contribution. Up to ≈ 4 ML thickness the interlayer distances are nearly constant. Above 4 ML thickness the interlayer distance rapidly increases. Between 6 and 9 ML the vertical interlayer distance stays again nearly constant, and is still below the value found for BCC(1 1 0) oriented 12 ML Fe/Cu(1 0 0) which, as shown in Fig. 4a, agrees very well with the value from literature for BCC bulk Fe(1 1 0). Nevertheless, the strong increase in $a_\perp$ of the Fe_xCo_{1-x} films above 4 ML thickness may serve as an indication for the affinity of the $Fe_{85}Co_{15}$ films towards forming the BCC(1 1 0) structure.

Finally, let us consider the results of the Kerr measurements, after briefly recalling the behavior of the saturation magnetization of the pure constituents Co and Fe as a function of film thickness. Whereas in Co films the whole film contributes to the Kerr signal indicating homogeneously magnetized film [13,14,24,40,41,62], the Kerr signal for Fe does not increase linearly with thickness. Instead, the Kerr signal drops by $\approx 50\%$ above ≈ 4 ML thickness, and stays nearly constant up to ≈ 10 ML thickness [11,12,18], where the martensitic transformation from FCC to BCC Fe sets in. This non-linear dependence of the Kerr signal on film thickness is connected to a relaxation of the lower lying layers in films above 4 ML thickness [33,34,38,43], which results in a film where only the topmost one or two atomic layers are ferromagnetically ordered [11,12,18]. Here we present measurements of the saturation Kerr signal of

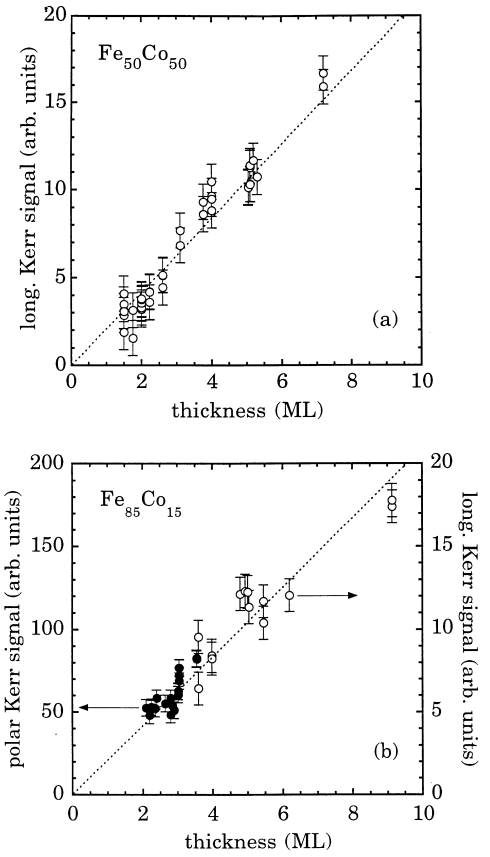

Fig. 5. Kerr signal measured in saturation as a function of film thickness. (a) $Fe_{50}Co_{50}$, longitudinal Kerr signal, (b) $Fe_{85}Co_{15}$, longitudinal (open symbols) and polar (filled symbols) Kerr signal. Because of the reorientation of the easy axis of magnetization at ≈ 3.5 ML, the scales for polar and longitudinal Kerr signals in panel (b) are chosen such that they coincide around 3.5 ML thickness.

Fe_xCo_{1-x}/Cu(1 0 0) as a function of film thickness in two different composition regions, namely (i) $Fe_{50}Co_{50}$, where we find smooth, nearly unstrained films with (1×1) LEED patterns, and (ii) $Fe_{85}Co_{15}$, where several superstructures are observed, and the roughness of the films as well as their vertical interlayer spacing increases rapidly above 4 ML thickness. The results are plotted in Fig. 5a for $Fe_{50}Co_{50}$ and Fig. 5b for $Fe_{85}Co_{15}$ films. In $Fe_{50}Co_{50}$ we observe a linear increase of the longitudinal Kerr signal with thickness, which implies that the whole film equally contributes to the magnetization. The more interesting case are the $Fe_{85}Co_{15}$ films, displayed in Fig. 5b. At that composition a spin reorientation transition from out-of-plane to in-plane with increasing film thickness is observed. This spin reorientation transition does not only occur as a function of film thickness, but also as a function of alloy composition, and of temperature. It has been the topic of a recent publication [50], so that here we restrict ourselves to a short summary of the results. Above $\approx 75\%$ Fe content the easy direction of magnetization switches from in-plane at lower Fe concentrations to out-of-plane at higher Fe concentrations at film thicknesses between 2 and 3.5 ML. The actual concentration at which the spin reorientation transition occurs is a function of film thickness, or vice versa, in the sense that a larger Fe content shifts the spin reorientation transition to higher film thicknesses. In $Fe_{85}Co_{15}$ films (Fig. 5b) the reorientation of the easy direction of magnetization at room temperature occurs at ≈ 3.5 ML thickness [50]. Therefore, in Fig. 5b for films below this thickness the polar Kerr signal is plotted, along with the longitudinal Kerr signal for films above this thickness. Since the magnitude of the Kerr signal in polar and longitudinal geometry differs strongly [63], the longitudinal and polar Kerr signals found close to the critical thickness were used to align the scales of both in order to plot them into the same graph. Surprisingly, also for $Fe_{85}Co_{15}$ a linear increase of the Kerr signal is found. This behavior is different from that of pure Fe films on Cu(1 0 0) and reflects the absence of a structural transformation to an unstrained FCC lattice in Fe_xCo_{1-x} films.

4. Discussion

To facilitate the discussion of the results, we summarize the experimental findings obtained with the different techniques in Fig. 6 in the form of schematic phase diagrams. In panels (a) through (d) the results from MEED, LEED, LEED–$I(E)$, and MOKE measurements, respectively, are reproduced as a function of both Fe concentration x (abscissa) and film thickness d (ordinate).

The line shown in Fig. 6a approximately separates regions in concentration-thickness space with

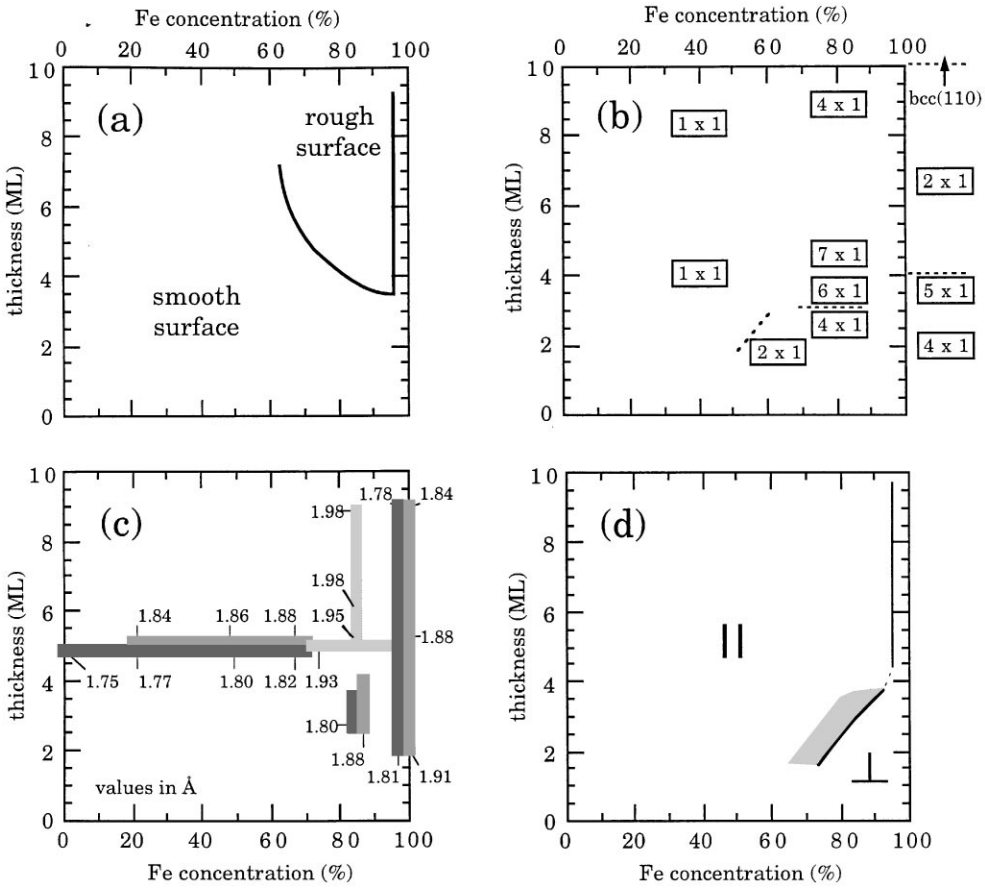

Fig. 6. Schematic summary of the experimental results in the form of concentration-thickness phase diagrams. (a) Results from MEED measurements. The line approximately separates regions with high specular MEED intensity, smooth surface, from regions with low specular MEED intensity, rough surface (cf. Fig. 1). (b) Appearance of LEED superstructures. The labels outside the right-hand side of the graph correspond to the superstructures found in pure Fe films. (c) Result of a kinematic analysis of LEED–$I(E)$ curves. Different vertical interlayer distances are reproduced in a grayscale, where brighter shades of gray correspond to larger interlayer distances. Numbers indicate values in Å. (d) Magnetic anisotropy: the line separates regions of perpendicular ($\perp$) and in-plane magnetic anisotropy ($\parallel$) at room temperature (cf. Ref. [50]). The shaded region represents the area in which at 120 K in addition films are perpendicularly magnetized.

high specular MEED intensity, i.e., smooth surface, from regions with low specular MEED intensity, i.e. rough surface (cf. Fig. 1). This division is also supported by the behavior of the diffuse LEED intensity background. Panel (b) summarizes the different superstructures observed in the LEED patterns. The labels outside the right-hand side of the graph correspond to the superstructures found in pure Fe films. The results of the simple kinematic analysis of the LEED-$I(E)$ curves are presented in Fig. 6c. Here the different values of the vertical interlayer distance are reproduced in a grayscale, where brighter shades of gray correspond to larger interlayer distances. Additionally, numerical values for the average interlayer distance in Å are indicated at several points in concentration-thickness space. Panel (d) indicates regions of perpendicular and in-plane magnetic anisotropy, as presented in Ref. [50]. The line in the phase diagram marks the border between regions in which the easy axis of

magnetization at room temperature lies in the plane of the film (∥) or is aligned perpendicular to the plane of the film (⊥). The shaded region represents the area in which the easy axis of magnetization depends on temperature: Films within that area are perpendicularly magnetized at 120 K, whereas at room temperature they are in-plane. The spin-reorientation transition as a function of both film thickness and composition is a result of the magnetic anisotropy decreasing from pure Fe films to $Fe_{70}Co_{30}$. The vertical line at the right-hand side of the diagram represents the fact that for all investigated films of these thicknesses pure Fe films showed a perpendicular magnetization, whereas films with the smallest Co content had their magnetization already in the plane of the film. For films below ≈ 1.5 ML the Curie temperature is below the cryogenic temperature limit of our setup (≈ 120 K).

When comparing panels (a)–(c) of Fig. 6 it becomes obvious that the region in which rough film surfaces are encountered is the one in which films have the highest vertical atomic distances. In addition, all these films show superstructures in the LEED diffraction pattern. These superstructures are observed neither in pure Fe films, nor in FeCo alloy films with lower Fe content. At lower film thicknesses below ≈ 3 ML superstructures similar to pure Fe films are observed, if the Fe concentration is higher than $\approx 60\%$. Generally, in FeCo films the formation of superstructures, i.e. of surface reconstructions, seems to be correlated to a high vertical interlayer distance.

Let us therefore now focus on the development of the vertical interlayer distance $a_\perp$ with Fe concentration x. Pure Co films of 5 ML thickness exhibit a value of $a_\perp$ of 1.75 Å, which translates into an $\approx 3.8\%$ vertical contraction with respect to the Cu lattice. This is a consequence of the in-plane tensile strain introduced by the Cu substrate having a larger lattice constant than FCC Co. Upon adding some Fe to have low Fe concentration FeCo alloy films, this value of the vertical interlayer distance increases, which means that the strain is partially relaxed, assuming a cubic unit cell of the FeCo alloy films. Obviously, the equilibrium FCC lattice parameter of the FeCo films is getting closer to the Cu lattice parameter upon incorporation of Fe atoms. Additionally, some layers at the surface show the expanded interlayer distance, as discussed in the previous section, which is already larger than the Cu lattice parameter (upper bar at 5 ML in Fig. 6c). Both vertical interlayer distances increase with increasing Fe concentration x up to about $x = 70\%$. This reflects the behavior of the lattice parameter of bulk FeCo, where for both FCC and BCC structures also an increase of the lattice parameter with increasing Fe content is encountered (cf. Fig. 4a) [60]. At 70% Fe content $a_\perp$ of the lower layers reaches that of the substrate, which means that the lateral tensile strain present in pure Co films has disappeared by alloying more and more Fe into the films. Judging from the lattice expansion relative to the substrate in the vertical direction, the in-plane strain in extrapolation would be converted into a compressive strain beyond $x = 70\%$. Starting at exactly that concentration a discontinuous jump of the vertical atomic distance to 1.93 Å occurs for both the upper and lower layers. This is correlated to the transition to a rough film surface, as concluded from MEED specular beam and LEED background intensity (Fig. 6a), and the appearance of LEED superstructures (Fig. 6b).

In the following we will propose an explanation of that behavior. For this we need to assume that the equilibrium crystalline structure of the FeCo alloy films on FCC Cu(1 0 0) is also FCC. Then we are able to distinguish between compressive and tensile strain by comparing the lateral and vertical lattice constants in the films. The reaction of the structure in a thin film to both types of strain can be very different. In a thin film the strain is introduced by the lattice mismatch between the film and a substrate. This means that the force acts only in the plane of the film, whereas in the direction perpendicular to the plane the film just reacts to this external force in order to minimize the total energy of the substrate–film system. The difference between compressive and tensile lateral strain is based on the different ways the minimum in total energy can be achieved. A film which is expanded in the plane, like, e.g., Co/Cu(1 0 0), may reduce the vertical layer spacing to minimize the total energy. Any kind of additional corrugation would lead to a further increase of the atomic distances, and

hence of the energy. Therefore, for example, Co films on Cu(1 0 0) stay fixed in their unreconstructed but tetragonally distorted FCC structure. Ferromagnetic FCC Fe, on the other hand, with an extrapolated room temperature lattice constant of 3.65 Å [64], is already slightly compressed in the film plane when grown epitaxially on Cu(1 0 0). Such laterally compressed films, in contrast to laterally expanded films, have the opportunity to decrease the overall energy further by building up a vertical corrugation in addition to a vertical expansion. A corrugation is achieved by displacing some atoms out of their atomic planes, which results in an increased spacing between these atoms and the adjacent atomic planes. As a result, the mean interatomic distance increases. Such an interpretation would be consistent with the structure of FM FCC Fe/Cu(1 0 0) films, which show a complicated superstructural corrugation as revealed by Müller et al. [34]. In contrast, no superstructures were observed in FM FCC Fe films on Cu_3Au(1 0 0) [7]. This absence of superstructures on the Cu_3Au substrate, which has a 3.9% larger lattice constant than Cu leading to laterally expanded Fe films, is also explained within that argumentation.

As long as we have tensile strain, we would therefore not expect strong changes in the geometric structure of the films, except for a reduction of the tetragonal distortion with decreasing strain. But switching from tensile to compressive strain, when the equilibrium lattice constant of the film exceeds the lattice parameter of the substrate, some corrugation can be expected. In FeCo/Cu(1 0 0) this happens around $x = 70\%$, and indeed the onset of the appearance of superstructures is observed. The relation between the lattice parameter of the FeCo films and the Cu substrate may thus account for the division of the phase diagram (Fig. 6a) into the two morphological regions: Region I with $x < 70\%$, which is governed by tensile lateral strain, resulting in smooth films, and region II with $x > 70\%$, which is governed by compressive lateral strain, resulting in a corrugated film. It is the continuous variation of the lattice parameter through the continuous variation of the alloy composition, that in the system Fe_xCo_{1-x}/Cu(1 0 0) allows one to observe such general trends in the interrelation between structural and morphological properties in epitaxial growth. As long as the epitaxial relation of FeCo to the Cu substrate is such that the films are under tensile strain, the growth mode is layer-by-layer, and the films exhibit smooth surfaces. As soon as the strain becomes compressive, the layer-by-layer growth is restricted to the first three monolayers, and superstructures occur; exceeding that thickness, films develop a high surface roughness. It should be also emphasized that in the intermediate strain region ($50\% < x < 70\%$) the films reveal a partial relaxation at the vacuum interface. Layers with different vertical strain exist thus within the same ferromagnetic film, in the same way as it happens for the room-temperature grown Fe/Cu(0 0 1) between 4 and 10 ML thickness [33,34].

The magnetic behavior of the FeCo/Cu(1 0 0) films (cf. Fig. 6) differs strongly from that of room-temperature grown FCC Fe films on Cu(1 0 0). In the latter a thickness region (5–11 ML) with a small and constant magnetic saturation is found [11,12,18]. This is correlated to a structure with a vertically expanded top layer on relaxed underlayers. The latter are assumed to be antiferromagnetically ordered, with a Néel temperature of 70 K [42] thus giving rise to the observed low overall ferromagnetic moment of the films, which is carried by the expanded top layers. The correlation between structure, or more specifically the atomic volume, and the presence of different magnetic phases is held responsible for that behavior [65,66]. On the contrary, in the Fe_xCo_{1-x} films we did not observe any indication for an other than linear dependence of the MOKE saturation signal with film thickness.

The interesting question is now why a comparable phase with concurrent ferromagnetic and antiferromagnetic[1] regions is absent in Fe_xCo_{1-x}/Cu(1 0 0) for $x < 100\%$. To address that point, we will compare three thin film systems on Cu(1 0 0): pure Fe films grown at LT, pure Fe films grown

[1] We refer to the state as antiferromagnetic for reasons of clarity, although it appeared nonmagnetic in our experiments due to the low-temperature limitation of our set-up.

at RT, and Fe_xCo_{1-x} films with $70\% \leqslant x < 100\%$, also grown at RT.

Up to about 4 ML thickness the structure of all of the three considered films is very similar, characterized by an expanded vertical interlayer distance in all layers, and the typical superstructures [18,31,32,34]. When exceeding 4 ML, this expanded FCC structure becomes unstable, and a structural transformation, which is different for the three cases, occurs. Whereas the RT grown FCC Fe films show the relaxed antiferromagnetic FCC structure with an expanded ferromagnetic top layer, the LT grown Fe films undergo a transformation to a BCC(1 1 0) structure with pronounced diffraction spots between 3.2 and 5.8 ML [5]. The Fe_xCo_{1-x} films show a further vertical expansion, but not yet a transformation to the BCC(1 1 0) structure. One of the possible reasons for the different behavior may be the morphology of the films. As was shown by STM, the RT grown Fe films consist of quite large islands with a diameter in the order of 20 nm, as compared to around 2 nm in the case of LT grown Fe films [36]. During the transition from the expanded FCC structure to the BCC(1 1 0) structure the films have to overcome a potential barrier in order to be able to restructure, which includes a further increase of the vertical interlayer spacing. This barrier is lower for films consisting of small islands, because lateral relaxations at the island borders provide an effective strain relief mechanism. This lets one conclude that the large FCC islands of RT grown Fe have a stabilizing effect, making it energetically more favorable to assume the relaxed FCC structure with an expanded overlayer than to directly transform into the BCC(1 1 0) structure, like the LT grown Fe films do. It has been discussed that also the so-called BCC-precipitates may play some role in the stabilization of the FCC phase of RT grown Fe [36]. These BCC-precipitates are small regions the structure of which differs from the surrounding FCC areas, and which have already been found at thicknesses lower than 5 ML [10,36]. Because of their different crystalline structure they might act as dislocations, facilitating the strain relief and thus lowering the energy of the FCC structure. Nevertheless, also the RT grown Fe films transform to the BCC(1 1 0) structure after exceeding a thickness of ≈ 10 ML. The number of the BCC-precipitates increases with the thickness of the films, the regions between them still keeping the FCC structure, but the size of the connected FCC regions becoming smaller in lateral direction [10,36]. At a thickness of ≈ 10 ML a sudden transformation of the remaining FCC areas to the BCC(1 1 0) structure occurs. This is probably related to the point where the connected FCC areas, separated by BCC precipitates, are becoming too small to resist the transformation to the BCC(1 1 0) structure. This model implies that one of the necessary conditions for the existence of the FCC structure with concurrent ferromagnetic and antiferromagnetic regions is that continuous regions of the FCC structure, exceeding a certain critical size, exist.

No direct information concerning the size of the islands of Fe_xCo_{1-x} films is available at present. But from the MEED intensity oscillations of RT grown Fe films and RT grown Fe_xCo_{1-x} films, as well as from the background intensity of the LEED patterns, which both are practically identical up to a thickness of 3 ML, we can conclude that the island size of the Fe_xCo_{1-x} films must be very similar to that of RT grown Fe films. Nevertheless, the Fe_xCo_{1-x} films do not transform to a structure with relaxed FCC underlayers and an expanded overlayer. This lack of a structural rearrangement has to be a consequence of the presence of Co atoms in the films. Possible reasons can be: first, the different 'size' of the Co atoms, and second, their magnetic moment, which is lower than that of ferromagnetic FCC Fe [66]. The 'size' of the Co atoms may prevent large FCC Fe islands already at the initial stages of growth. For an $Fe_{90}Co_{10}$ film the average distance of Co atoms dispersed in the Fe matrix will be around 15–20 Å. One can imagine that around each Co atom there is a local strain field which blocks a structural rearrangement. The difference in 'size' between Fe and Co atoms, however, is not very large. Therefore, we have to consider also the second possibility, the magnetic moment of the Co atoms. As measurements of the magnetic circular dichroism have shown [67–71], for Fe_xCo_{1-x} films the magnetic moment of the Co atoms aligns ferromagnetically with the magnetic moment of the Fe atoms. When transforming to the

relaxed FCC structure, the underlayers in RT grown Fe films lose their ferromagnetic properties by assuming the lower atomic volume antiferromagnetic state. The presence of randomly distributed Co moments in the matrix of FCC Fe could prevent this transition due to magneto-volume effects. Further insight into the microscopic mechanism of the structural stabilization requires the following question to be answered: how much Co is needed to achieve a stabilization of the ferromagnetic state? This clearly demands investigations on films in the dilute alloy limit which are not available at present.

Despite of the above mentioned the Fe_xCo_{1-x} films do not reach the BCC structure. Whereas the RT and LT Fe films transform to BCC in a small thickness range of about 1.5 ML, the structure of 9 ML thick Fe_xCo_{1-x} films is still relatively far away from BCC(1 1 0), although the vertical interlayer distance already starts to increase above 4 ML thickness. This obviously means that introducing Co atoms into the pure Fe films not only prevents the transformation to the relaxed FCC structure, but also hinders the transformation to the BCC structure, keeping the film in a strongly distorted FCC arrangement.

Finally, we turn to the spin reorientation transition. In contrast to the distinct mutual interactions between structure and magnetism found for other magnetic properties, the spin reorientation transition seems not to be connected to any structural properties. In fact, from comparison of Fig. 6d with Figs. 6a–c no obvious correlation of the spin reorientation transition from perpendicular to in-plane magnetic easy axis with a transition in structural or morphological properties can be seen. Both the vertical lattice parameter and the LEED superstructure do not change at the line which separates in-plane and out-of-plane magnetization. This means the reorientation transition is neither caused by a structural change, nor does it cause a change in the structural parameters. We thus attribute this spin reorientation transition as being solely due to changes in the electronic properties. The tiny differences in the average d-band occupation number according to the alloy composition cause a change in the magnetic anisotropy energy and thereby a spin reorientation transition [50].

5. Summary

Summarizing we have shown by the example of Fe_xCo_{1-x} films on Cu(1 0 0) that the morphology, the structure, and the magnetism of heteroepitaxial ferromagnetic films are closely linked. Over the whole thickness range investigated the Fe_xCo_{1-x} films grow in an FCC-like structure. The morphology, the superstructures, and the vertical interlayer distance of the films depend on their composition and thickness. Films with less than 60–70% Fe grow in a layer-by-layer mode as smooth films, and show a (1×1) LEED pattern. Films of 5 ML thickness in this concentration range (except pure Co films) show two different vertical interlayer distances. Both depend on the film composition, and increase towards higher Fe concentrations. The larger vertical interlayer distance can be related to the vacuum side of the film. Segregation of one of the constituents either laterally or vertically could be excluded. Films with more than 60–70% Fe show several different LEED superstructures depending on the thickness. For Fe_xCo_{1-x} films with $70\% \leqslant x < 100\%$ below ≈ 3.5 ML thickness the superstructures as well as the morphology and the interlayer distances are virtually the same as for pure Fe films, the latter being expanded relative to the Cu substrate. Above this thickness the Fe_xCo_{1-x} films with $70\% \leqslant x < 100\%$ become rough, the interlayer distance further increases, and the observed LEED superstructure differs from that of pure Fe films, still being significantly different from that of the BCC(1 1 0) structure observed for pure Fe films above ≈ 10 ML thickness. The relaxation from a fully expanded FCC structure below 4 ML to a relaxed FCC underlayer with expanded overlayer between 4 and 10 ML observed in pure Fe films is not observed in Fe_xCo_{1-x}. The dependence of the film properties on the composition can be linked to the strain provided by the substrate. Below 60–70% Fe the expansion of the FCC structure in the plane of the film stabilizes this structure resulting in smooth films with (1×1) LEED pattern. Above this Fe concentration the films become compressed in the plane of the film. This energetically favors corrugated films, unstable with respect to structural transitions. We believe that in Fe_xCo_{1-x} films with $70\% \leqslant x < 100\%$ the

absence of the relaxed FCC phase, as it is observed in pure Fe films grown at RT, is caused by the Co atoms acting as defects in the FCC structure in a geometrical, but more important in a magnetic sense, concerning the presence of Co atoms in an antiferromagnetically ordered relaxed underlayer. This missing structural relaxation above 4 ML thickness results in a linear increase of the Kerr signal with thickness for these films, as also observed for the Fe_xCo_{1-x} films below 60–70% Fe, as well as for pure Co films.

Acknowledgements

We are grateful for financial support by the BMBF under grant no. 05 621 EFA, and the DFG under grant no. Schn 353/3. We would like to thank J. Kirschner, W. Hübner, H.P. Oepen, and Y. Millev for fruitful discussions, and B. Zada for technical assistance. M.Z. thanks the Max-Planck-Gesellschaft for a stipend.

References

[1] J.A.C. Bland, B. Heinrich, (Eds.), Ultrathin Magnetic Structures, Vol. 1, Springer, Berlin, 1994.
[2] B. Heinrich, J.A.C. Bland (Eds.), Ultrathin Magnetic Structures, Vol. 2, Springer, Berlin, 1994.
[3] M. Zharnikov, A. Dittschar, W. Kuch, C.M. Schneider, J. Kirschner, Phys. Rev. Lett. 76 (1996) 4620.
[4] M. Zharnikov, A. Dittschar, W. Kuch, C.M. Schneider, J. Kirschner, J. Magn. Magn. Mater. 165 (1997) 250.
[5] H. Zillgen, B. Feldmann, M. Wuttig, Surf. Sci. 321 (1994) 32.
[6] M.-T. Lin, J. Shen, W. Kuch, H. Jenniches, M. Klaua, C.M. Schneider, J. Kirschner, Phys. Rev. B 55 (1997) 5886.
[7] M.-T. Lin, J. Shen, W. Kuch, H. Jenniches, M. Klaua, C.M. Schneider, J. Kirschner, Surf. Sci. 410 (1998) 290.
[8] J. Shen, P. Ohresser, C.V. Mohan, M. Klaua, J. Barthel, J. Kirschner, Phys. Rev. Lett. 80 (1998) 1980.
[9] C. Chappert, P. Bruno, J. Appl. Phys. 53 (1988) 5736.
[10] J. Giergiel, J. Shen, J. Woltersdorf, A. Kirilyuk, J. Kirschner, Phys. Rev. B 52 (1995) 8528.
[11] D. Li, M. Freitag, J. Pearson, Z.Q. Qiu, S.D. Bader, Phys. Rev. Lett. 72 (1994) 3112.
[12] D. Li, M. Freitag, J. Pearson, Z.Q. Qiu, S.D. Bader, J. Appl. Phys. 76 (1994) 6425.
[13] J.J. de Miguel, A. Cebollada, J.M. Gallego, S. Ferrer, R. Miranda, C.M. Schneider, P. Bressler, J. Garbe, K. Bethke, J. Kirschner, Surf. Sci. 211–212 (1989) 732.
[14] J.J. de Miguel, A. Cebollada, J.M. Gallego, R. Miranda, C.M. Schneider, P. Schuster, J. Kirschner, J. Magn. Magn. Mater. 93 (1991) 1.
[15] J. Shen, H. Jenniches, C.V. Mohan, J. Barthel, M. Klaua, P. Ohresser, J. Kirschner, Europhys. Lett. 43 (1998) 349.
[16] H. Jenniches, M. Klaua, H. Höche, J. Kirschner, Appl. Phys. Lett. 69 (1996) 3339.
[17] R. Allenspach, A. Bischof, Phys. Rev. Lett. 69 (1992) 3385.
[18] J. Thomassen, F. May, B. Feldmann, M. Wuttig, H. Ibach, Phys. Rev. Lett. 69 (1992) 3831.
[19] D.E. Fowler, J.V. Barth, Phys. Rev. B 53 (1996) 5563.
[20] S. Müller, P. Bayer, C. Reischl, K. Heinz, B. Feldmann, H. Zillgen, M. Wuttig, Phys. Rev. Lett. 74 (1995) 765.
[21] J.F. Cochran, W.B. Muir, J.F. Rudd, B. Heinrich, Z. Celinski, T.T. Le-Tran, W. Schwarzacher, W. Bennet, W.F. Egelhoff Jr., J. Appl. Phys. 69 (1991) 5206.
[22] P. Xhonneux, E. Courtens, Phys. Rev. B 46 (1992) 556.
[23] M. Kowalewski, C.M. Schneider, B. Heinrich, Phys. Rev. B 47 (1993) 8748.
[24] P. Krams, F. Lauks, R.L. Stamps, G. Güntherodt, Phys. Rev. Lett. 69 (1992) 3674.
[25] C. M. Schneider, A. K. Schmid, P. Schuster, H. P. Oepen, J. Kirschner, in: Magnetism and Structure in Systems of Reduced Dimension, Plenum Press, New York, 1993.
[26] E. Navas, P. Schuster, C.M. Schneider, J. Kirschner, A. Cebollada, C. Ocal, R. Miranda, J. Cerdá, P. de Andrés, J. Magn. Magn. Mater. 121 (1993) 65.
[27] J.R. Cerdá, P.L. de Andrés, A. Cebollada, R. Miranda, E. Navas, P. Schuster, C.M. Schneider, J. Kirschner, J. Phys.: Condens Matter 5 (1993) 2055.
[28] H. Li, B.P. Tonner, Surf. Sci. 237 (1990) 141.
[29] J. Fassbender, U. May, B. Schirmer, R.M. Jungblut, B. Hillebrands, G. Güntherodt, Phys. Rev. Lett. 75 (1995) 4476.
[30] W. Weber, A. Bischof, R. Allenspach, C.H. Back, J. Fassbender, U. May, B. Schirmer, R.M. Jungblut, G. Güntherodt, B. Hillebrands, Phys. Rev. B 54 (1996) 4075.
[31] K. Heinz, S. Müller, P. Bayer, Surf. Sci. 337 (1995) 215.
[32] S. Müller, P. Bayer, A. Kinne, C. Reischl, R. Metzler, K. Heinz, Surf. Sci. 331–333 (1995) 723.
[33] P. Bayer, S. Müller, P. Schmailzl, K. Heinz, Phys. Rev. B 48 (1993) 17611.
[34] S. Müller, P. Bayer, A. Kinne, P. Schmailzl, K. Heinz, Surf. Sci. 322 (1995) 21.
[35] P. Schmailzl, K. Schmidt, P. Bayer, R. Döll, K. Heinz, Surf. Sci. 312 (1994) 73.
[36] J. Giergiel, J. Kirschner, J. Landgraf, J. Shen, J. Woltersdorf, Surf. Sci. 310 (1994) 1.
[37] M. Wuttig, B. Feldmann, J. Thomassen, F. May, H. Zillgen, A. Brodde, H. Hannemann, H. Neddermeyer, Surf. Sci. 291 (1993) 14.
[38] M. Wuttig, J. Thomassen, Surf. Sci. 282 (1993) 237.
[39] H. Landskron, G. Schmidt, K. Heinz, K. Müller, C. Stuhlmann, U. Beckers, M. Wuttig, H. Ibach, Surf. Sci. 256 (1991) 115.
[40] C.M. Schneider, P. Bressler, P. Schuster, J. Kirschner, J.J. de Miguel, R. Miranda, Phys. Rev. Lett. 64 (1990) 1059.

[41] C.M. Schneider, P. Bressler, P. Schuster, J. Kirschner, J.J. de Miguel, R. Miranda, Vacuum 41 (1990) 503.
[42] R.D. Ellerbrock, A. Fuest, A. Schatz, W. Keune, R.A. Brand, Phys. Rev. Lett. 74 (1995) 3053.
[43] J.V. Barth, D.E. Fowler, Phys. Rev. B 52 (1995) 1528.
[44] M. Hansen, In: K. Anderko (Ed.), Constitution of Binary Alloys, McGraw-Hill, New York, 1958.
[45] E. Kneller, *Ferromagnetismus*, Springer, Berlin, 1962.
[46] D.I. Bardos, J. Appl. Phys. 40 (1969) 1371.
[47] M. Zharnikov, A. Dittschar, W. Kuch, K. Meinel, C.M. Schneider, J. Kirschner, Thin Solid Films 275 (1996) 262.
[48] J.G. Tobin, K.W. Goodman, G.J. Mankey, R.F. Willis, J.D. Denlinger, E. Rotenberg, A. Warwick, J. Appl. Phys. 79 (1996) 5626.
[49] J.G. Tobin, K.W. Goodman, G.J. Mankey, R.F. Willis, J.D. Denlinger, E. Rotenberg, A. Warwick, J. Vac. Sci. Technol. B 14 (1996) 3171.
[50] A. Dittschar, M. Zharnikov, W. Kuch, M.-T. Lin, C.M. Schneider, J. Kirschner, Phys. Rev. B 57 (1998) 3209.
[51] W. Kuch, A. Dittschar, K. Meinel, M. Zharnikov, C.M. Schneider, J. Kirschner, J. Henk, R. Feder, Phys. Rev. B 53 (1996) 11621.
[52] W. Platow, U. Bovensiepen, P. Poulopoulos, M. Farle, K. Baberschke, L. Hammer, S. Walter, S. Müller, K. Heinz, Phys. Rev. B 59 (1999) 12641.
[53] F. Baudelet, M.-T. Lin, W. Kuch, K. Meinel, B. Choi, C.M. Schneider, J. Kirschner, Phys. Rev. B 51 (1995) 12563.
[54] M. Salvietti, Xingyu Gao, private communication.
[55] U. Thomann, Ch. Reuss, M. Weinelt, and Th. Fauster, private communication.
[56] A. Zangwill, Physics at Surfaces, Cambridge University Press, Cambridge, 1988.
[57] M.P. Seah, W.A. Dench, Surf. Interface Anal. 1 (1979) 2.
[58] U. Gradmann, J. Magn. Magn. Mater. 100 (1991) 481.
[59] A.J. Freeman, R. Wu, J. Magn. Magn. Mater. 100 (1991) 497.
[60] W.B. Pearson, A Handbook of Lattice Spacings and Structures of Metals and Alloys, Vol. 1, Pergamon Press, Oxford, 1958.
[61] H.L. Davis, J.R. Noonan, J. Vac. Sci. Technol 20 (1982) 842.
[62] M.E. Buckley, F.O. Schumann, J.A.C. Bland, Phys. Rev. B 51 (1995) 6596.
[63] S.D. Bader, J. Magn. Magn. Mater. 100 (1991) 440.
[64] M. Acet, H. Zähres, E.F. Wassermann, W. Pepperhoff, Phys. Rev. B 49 (1994) 6012.
[65] V.L. Moruzzi, P.M. Marcus, K. Schwarz, P. Mohn, Phys. Rev. B 34 (1986) 1784.
[66] V.L. Moruzzi, P.M. Marcus, J. Kübler, Phys. Rev. B 39 (1989) 6957.
[67] Y.U. Idzerda, C.J. Gutierrez, L.H. Tjeng, H.-J. Lin, G. Meigs, C.T. Chen, J. Magn. Magn. Mater. 127 (1993) 109.
[68] S. Pizzini, A. Fontaine, E. Dartyge, C. Giorgetti, F. Baudelet, J.P. Kappler, P. Boher, F. Giron, Phys. Rev. B 50 (1994) 3779.
[69] L. Braicovich, C. Dallera, G. Ghiringhelli, N.B. Brookes, J.B. Goedkoop, Phys. Rev. B 55 (1997) R14729.
[70] R. Schellenberg, E. Kisker, M. Faust, A. Fanelsa, F.U. Hillebrecht, Phys. Rev. B 58 (1998) 81.
[71] E. Kisker, A. Faust, R. Schellenberg, A Fanelsa, F.U. Hillebrecht, J. Appl. Phys. 83 (1998) 7094.